RSC Advances

PAPER

View Article Online
View Journal | View Issue

Cite this: *RSC Adv.*, 2024, **14**, 14648

Photogalvanics of copper and brass working electrodes in the NaOH-Allura Red-D-galactose-DDAC electrolyte for solar power generation†

Pooran Koli * and Jyoti Saren

Solar energy is a limitless energy resource that can be used to produce electricity forever. Photogalvanic cells can convert solar energy into electricity with inherent power storage. The electrolyte(s) and a combination of two electrodes are the main materials required for fabrication of these cells. So far, platinum has been used as the working electrode in photogalvanic cells. Platinum is an extremely rare and expensive metal. Copper and its alloy (brass) have been identified as alternative working electrodes to substitute the platinum working electrode in photogalvanic cells. In addition, copper and brass utilization is identified to be an effective, user-friendly, and safe approach for high-power generation. Therefore, in the present work, cheap and easily obtainable copper and brass (alloy of copper and zinc) working electrodes have been exploited with the twin aim of high-power generation with less input cost. In the present study, the observed power, current, potential, and efficiency for the copper electrode are 552.3 μW, 4030 μA, 713 mV, and 8.54%, respectively, and those for the brass electrode are 546.4 μW, 5320 μA, 739 mV, and 6.12%, respectively. The observed electrical performance is greatly enhanced compared to most of the already reported photogalvanics with platinum electrode. Copper and brass are slightly and slowly corroded by the alkali, but despite this electrode loss, both materials are promising to produce the highest power. In the future, this electrode loss can be checked by using inhibitors.

Received 12th February 2024
Accepted 23rd April 2024

DOI: 10.1039/d4ra01091d

rsc.li/rsc-advances

1. Introduction

Solar energy is the radiant light and heat from the sun. Solar energy holds relevance and significance for human civilisation. Different techniques and appliances, such as photovoltaic cells,[1] perovskite solar cells,[2] organic solar cells (polymer solar cells),[3] dye-sensitized solar cells,[4] quantum dots,[5] photogalvanic cells,[6–8] *etc.*, are available for harnessing solar energy. Among all these techniques, the photovoltaic technique is commercially popular the world over for solar electricity generation. Its recent success as an economically viable source of electricity is founded on a simple optoelectronic device, the crystalline silicon solar cell.[9,10] The evolution of the crystalline silicon solar cell device is opening exciting opportunities. To realize the aim of practical application of the photogalvanic cells in daily life, the electrical output of these cells has to be further enhanced to a level at least comparable to that of the photovoltaic cells. The photogalvanic cell is a good approach for directly converting solar energy into electricity because these cells are simple and capable of producing solar energy with inherent storage capacity. Photogalvanic cells are electrochemical devices based on the photogalvanic effect. The photogalvanic cell technique consists of two dissimilar electrodes: a working electrode (usually platinum, Pt) that is exposed to light, and a counter electrode or reference electrode (usually a saturated calomel electrode, SCE) that is in the dark. The space between the electrodes is filled with a solution of photosensitizer (photon-absorbing species), reductant (electron-donating species) and surfactant (efficiency enhancer agent) in alkaline medium. The role of the working electrode in photogalvanic cells is to facilitate electron exchange between the semi/leuco reduced sensitizer molecule and external circuit. The counter electrode helps to complete the circuit and conducts the flow of current through the circuit.

In the beginning, photogalvanic researchers focused on using a coated Pt electrode with Fe^{2+} as a reducing agent.[7,8] Later on, they started using non-coated Pt electrode.[11–14] The reported electrical output for both coated and uncoated platinum electrodes was low. The comparatively low electrical cell performance of the photogalvanic cell was attributed to the large size of the Pt electrode (1 cm × 1 cm) with a saturated calomel electrode.[11–14] The photogalvanic cell's electrical performance was relatively low until the researchers started employing a small-sized Pt electrode in place of the large-sized Pt electrode.[15–18] The diffusion-controlled photogalvanic cells rely on ion diffusion throughout the bulk of the electrolytic solution. Therefore, one of the primary factors influencing the

Department of Chemistry, Jai Narain Vyas University, Jodhpur-342033, Rajasthan, India. E-mail: poorankoli@yahoo.com; saren2jyoti@gmail.com

† Electronic supplementary information (ESI) available. See DOI: https://doi.org/10.1039/d4ra01091d

electrodes' efficiency is the diffusion of ions. Thus, in order to obtain optimal diffusion, researchers focused on using a small Pt electrode with SCE, which less hinders the ion mobility and successfully enhances the photogalvanic performance. The Pt electrode presents itself as an excellent option as an inert electrode because of its superior ability to facilitate electron exchange. No other metal is able to make such claims. Therefore, the platinum electrode has been widely explored as a working electrode in photogalvanic cells. However, it is highly expensive and not available easily in the local market. Its procurement is very costly and time-consuming. In contrast, copper metal and brass alloy materials are cheap and easily available, even at the household level. Therefore, procuring copper metal and brass alloy is cheaper and less time consuming. One additional advantage of copper and brass is that the electrical output for the copper- and brass-based cells is relatively higher than that for platinum electrode-based cells.

From this literature survey, it is observed that researchers have focussed mainly on the costly and non-ubiquitous small platinum working electrode for enhancing the working efficiency of photogalvanic cells. Gangotri and Meena,[11,12] Madhwani *et al.*,[13] and Pramila and Gangotri[14] have exploited the platinum electrode (1 cm × 1 cm) in photogalvanic cells for solar energy conversion and storage.

There has been a research gap in neglecting the chemical diversity of the working electrodes (*e.g.*, the use of copper and brass). To have good conversion efficiency, the working electrode material should have more sites to receive electrons from the semi/leuco reduced sensitizer molecule and, in turn, facilitate movement of electrons towards the external circuit. This property of electrodes is dependent on the chemical nature of the material constituting the electrode. In the present work, in using copper and brass working electrodes instead of platinum electrode in the photogalvanic cell, there are many advantages. Firstly, the cost of the photogalvanic setup would be reduced if copper and brass electrodes are used instead of platinum electrodes because platinum electrodes are more expensive and non-ubiquitous. In the Indian market, platinum costs ~30 USD per g, but copper and brass are ubiquitous and more affordable at USD 8.56 per kg and USD 3.83 per kg, respectively. Copper and brass are also readily available in household materials and scraps, but platinum is more difficult to obtain. Secondly, copper and brass are active electrodes, which means copper and brass electrodes are more likely to react with the electrolyte and undergo chemical changes; they will also contribute in the photocurrent generation through the thermal process, whereas platinum is an inert electrode. The contribution of platinum is only for the exchange of electrons. Lastly, copper and brass electrodes may also have different electrochemical properties compared to platinum electrode, which would affect the efficiency and kinetics of the electrolysis process. Overall, while copper and brass electrodes can be used in photogalvanic cells, they may result in different outcomes compared to using platinum electrodes, particularly in terms of cost and electrical output. The electrochemical behavior of copper also has been of considerable interest in many areas of technology, including solar cell technology—such as in organic solar cells;[19] photovoltaic cells,[20] integrated circuits[21] and heat exchangers,[22] but there is no reported study on using copper and brass (copper alloy) as working electrodes in photogalvanic cells.[23–25]

Therefore, in the present study, copper and copper alloy (brass) electrodes of different dimensions have been exploited as the working (anodic) electrode along with graphite electrode as the counter (cathodic) electrode, with Allura Red as photosensitizer, D-galactose as reductant, and didecyl dimethyl ammonium chloride as surfactant in alkaline medium. In the present research, the novel electrode materials (copper and brass) have been used with the hope to further improve the electrical performance of the photogalvanic cell.

2. Material and methods

2.1. Chemicals used

Allura Red was used a photosensitizer. D-Galactose, didecyl dimethyl ammonium chloride and NaOH were used as reductant, surfactant, and alkaline medium, respectively. The stock solutions of Allura Red dye (M/500), D-galactose (M/100), didecyl dimethyl ammonium chloride (M/10) and NaOH (1N) have been prepared in singly distilled water. To keep the colored stock solution safe from light, it was stored in a dark container. Here, 'M' stands for molarity, which is defined as the number of moles of dissolved solute in one liter of the solution.

2.2. Preparation of stock solutions

Allura Red (M/500): 50 ml of M/500 Allura Red stock solution was prepared by dissolving 0.612 g of Allura Red in 50 ml of deionized water.

D-Galactose (M/100): 50 ml of M/100 D-galactose stock solution was prepared by dissolving 0.90 g of D-galactose in 50 ml of deionized water.

Didecyl dimethyl ammonium chloride (DDAC) (M/10): 50 ml of M/10 DDAC surfactant stock solution was prepared by dissolving 1.810 ml of DDAC surfactant in 50 ml of deionized water.

NaOH (1 M): 250 ml of 1 M of NaOH stock solution has been prepared by dissolving 15 g of NaOH pellets in 250 ml of deionized water.

An entirely new and unexplored combination of Allura Red as photosensitizer, D-galactose as reductant and didecyl dimethyl ammonium chloride (DDAC) as surfactant was tried in the present work. Allura Red is an azo dye, anionic in nature, and highly soluble in water (22 g/100 ml at 25 °C). Allura Red dye was used in this work due to its very high solubility in water, good absorbance in the visible region (501–507 nm) and efficient light-harvesting property.

DDAC was used as a surfactant in the present work due to its cationic nature. DDAC is a nonvolatile and photolytically stable salt that is highly soluble in water.[26]

The use of anionic Allura Red dye and cationic DDAC surfactant is supposed to serve as a very suitable dye-surfactant anionic–cationic pair for solar energy conversion and storage through the photogalvanic cells.

It has been reported in the literature that dye and surfactant molecules with opposite charges form a stable dye-surfactant complex in which the dye molecule is surrounded by surfactant micelles in some regular geometry, which retards intermolecular twisting and results in an enhancement of fluorescence.[27]

Further, there are no reports on D-galactose as a reductant in photogalvanic cells. D-Galactose is a reducing sugar that is capable of acting as a good reducing agent. In an alkaline solution, a reducing sugar forms some aldehyde or ketone, which allows it to act as a good reducing agent.

Alkaline medium NaOH was used in the present work because dye stability, dye solubility, and the dye's electron-donating tendency depends on the strength of the alkali medium of the electrolyte. Further, cell performance is poor in acidic medium. The low ability of the dye and reductant to donate electrons to platinum could be caused by proton attachment to the heteroatom and double bonds in the dye and reductant. This effect is not present in alkali media; the anion formation of dye and reductant enhances their electron-donation power. Therefore, in the present paper, the photogalvanics of an entirely new electrolyte of Allura Red (dye sensitizer), D-galactose (reductant), and didecyl dimethyl ammonium chloride (DDAC, as surfactant) in alkaline medium (NaOH) was studied. The unexplored combination of Allura Red-D-galactose-DDAC-NaOH with these characteristics have encouraged the authors to use these chemicals for further enhancing the electrical output of photogalvanic cells.

2.3. Electrodes used

Copper metal (Cu) and brass (alloy of copper and zinc) were used as working electrodes. Graphite has was used as counter electrode; it is inert in nature and has a wide range of possible uses, including energy storage and conversion. It is good for the environment because graphite electrodes do not need to be changed regularly, with their long operating life and easy availability in batteries.

2.3.1. Preparation of copper and brass electrodes. Two sizes of copper electrodes (*i.e.*, 0.3 cm × 0.2 cm × 0.05 cm, and 1.0 cm × 1.0 × cm × 0.05 cm) were used. From the market, a large copper sheet of thickness 0.05 cm was purchased. From this copper sheet, copper electrodes of the required dimensions were cut and used. Two sizes of brass electrodes (*i.e.*, 0.3 cm × 0.2 cm × 0.05 cm, and 1.0 cm × 1.0 × cm × 0.05 cm) were also used. Similarly, from the market, a large brass sheet of thickness 0.05 cm was purchased. From this brass sheet, brass electrodes of the required dimensions were cut and used. Similarly, the platinum electrode was also prepared. Further, in this research, the combined surface area of all six faces of an electrode was assumed to be the active surface area of the electrodes. For electrodes of 0.3 cm × 0.2 cm × 0.05 cm and 1.0 cm × 1.0 × cm × 0.05 cm dimensions, the active electrode area was considered as 0.17 cm^2 and 2.2 cm^2, respectively.

2.4. Apparatus used

The present research used the following apparatus: two digital multimeters (model-DT830D UNITY), one for measuring potential in millivolts and another for measuring current in microamperes; copper connecting wires (to make circuit wires); a rheostat/potentiometer Elcon B 1M 1706 (to change the circuit's resistance); a brass plug circuit key (to close the circuit); a 200 watt Philips bulb (as an illuminating source); a HTC LX-101A Luxmeter (±5 percent of the reading, to measure the illumination intensity); a digital pH meter (Nexqua company, to measure pH of the electrolyte solution); and a water quality test meter C-100 for measuring various physical parameters of the solution, including total dissolved solids (TDS), electrical conductivity (EC), temperature (TEMP), seawater gravity (S.G.), and salt.

2.5. Experimental setup, experimental method and calculation formula

A very simple experimental setup was used in the present research work, consisting of a light source (200 watt Philips bulb), two digital multimeters (DT830D UNITY) to measure the current and potential, a rheostat/potentiometer Elcon B 1M to adjust the resistance of the circuit, a circuit key, and an externally blackened H-shaped glass tube with a diffusion length of 4.5 cm. One arm of the H-shaped glass tube has a transparent window for illumination to act as an illuminated chamber, and the other arm, without a window, acts as the dark chamber.[28–30] Chemically different types of working electrodes (copper metal and brass of different dimensions) were used as working electrode (as negative terminal, anodic). A graphite electrode (cylindrical shape, length 4.1 cm × diameter 0.3 cm) was used as counter electrode (as positive terminal, cathodic) (Fig. 1). The working electrode was dipped in the illuminated chamber against the window. The graphite electrode was immersed in the dark chamber.

During the experiment, a complete electrolyte solution consisting of Allura Red (photosensitizer), D-galactose (reductant), DDAC (surfactant) and sodium hydroxide was put into the H-cell, and then a stable potential (called dark potential, V_{dark}) is observed in the dark while the circuit is open. The bulb is then turned on, and the copper/brass electrode (whichever is employed in the experiment as a working electrode) becomes illuminated. A rise in potential is then noticed at a regular interval of time. There is a sudden jump in the potential (called maximum potential, V_{max}), and after that, the potential gradually goes down to a relatively stable potential (called open-circuit potential, V_{oc}). In order to observe the maximum current (I_{max}) at zero external resistance (load), the circuit is then closed using the circuit key. After some time, the current gradually decreases to equilibrium current (I_{eq}, also called short-circuit current, I_{sc}). The potential at I_{sc} is nearly zero. To study the *I–V* characteristics of the cell, the resistance of the circuit was adjusted using a potentiometer/rheostat from minimum to maximum. The power corresponding to the highest value of the product of '*I*' and '*V*' is called power at power point (P_{pp}), or maximum power.[31] The potential corresponding to this P_{pp} is the potential at power point (V_{pp}), and the current corresponding to this P_{pp} is current at power point (I_{pp}). Cell performance is determined by calculating the

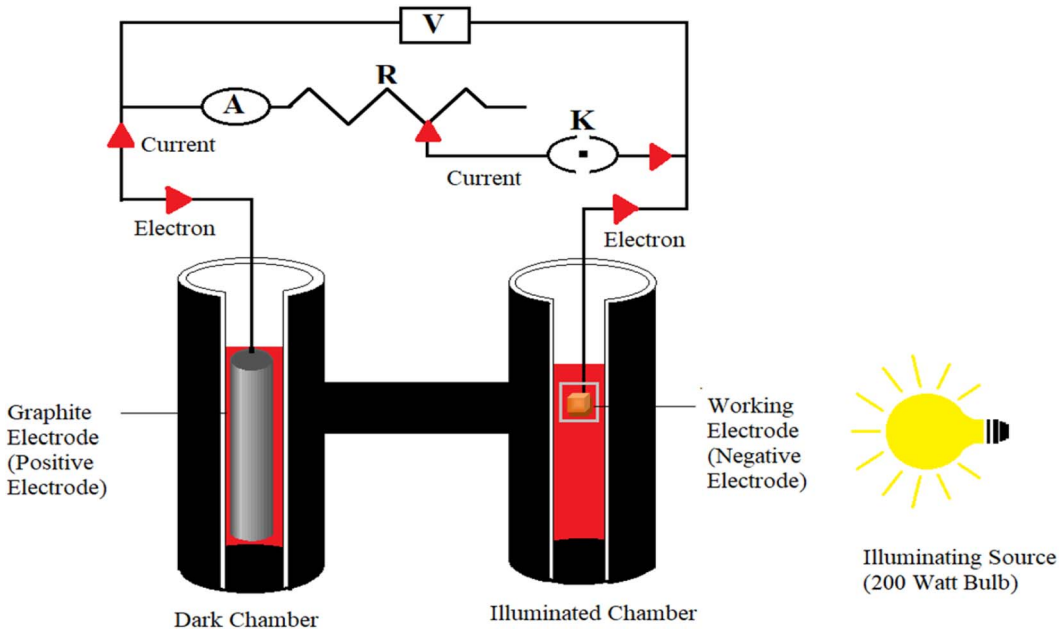

Fig. 1 Experimental setup of a photogalvanic cell (*A*, a digital multimeter used as ammeter; *V*, another digital multimeter used as voltmeter; *R*, a potentiometer/rheostat; *K*, key).

conversion efficiency (CE), fill factor (FF), and storage capacity (in terms of the half change time, $t_{0.5}$).

The FF and CE are calculated as FF = $(P_{output})/(V_{oc} \times I_{sc})$, CE = $(P_{output} \times 100\%)/(P_i \times A)$, and CE = $(FF \times V_{oc} \times I_{sc} \times 100\%)/(P_i \times A)$, respectively, where '$P_i$' and '$A$' represent the illumination intensity in mW cm^{-2}, and the total surface area of all six faces of the Pt electrode are in cm^2, respectively. Further, the V_{max} and I_{max} are positively related with CE; thus, CE will be higher when the values of V_{max} and I_{max} are higher.

For all classes of solar cells (*e.g.*, photovoltaic cells, dye-sensitized solar cells, perovskite solar cells, *etc.*), the CE and FF values are concordant (if CE is high then FF is also proportionately high). However, for the photogalvanic cells as in the present study, the CE is high, but FF is not proportionately high. For photogalvanic cells, it may be attributed to photodecay of the dye photosensitizer, the short life of excited states of the dye photosensitizer, and the diffusion requirement of photosensitizer molecules, *etc.*[15]

3. Mechanism of photogeneration of current in the photogalvanic cell

The photopotential and photocurrent generation in the photogalvanic cell can be explained by the following mechanism:[32–34]

1st Step: photophysical processes in the illuminated chamber: on illumination, the dye molecule (*e.g.*, Allura Red or any other sensitizer molecule) gets excited. The excited dye molecule accepts an electron from the reductant (D-galactose) and is converted into the semi or leuco form of the dye.

$$\text{Allura Red} \xrightarrow{h\nu} \text{Allura Red*}\ (\text{S}) \xrightarrow{I_{sc}} \text{Allura Red*}\ (\text{T}) \quad (1)$$

$$\text{Allura Red*}\ (\text{T}) + (\text{D-galactose}) \rightarrow \text{Allura Red}^{-}\ (\text{semi or leuco}) + \text{D-galactose}^{+} \quad (2)$$

2nd Step: photophysical processes at the working electrode: at the working electrode, the semi or leuco form of the dye molecules loses an electron and is converted into the original dye molecule.

$$\text{Allura Red}^{-} \rightarrow \text{Allura Red} + e^{-}\ (\text{at working electrode}) \quad (3)$$

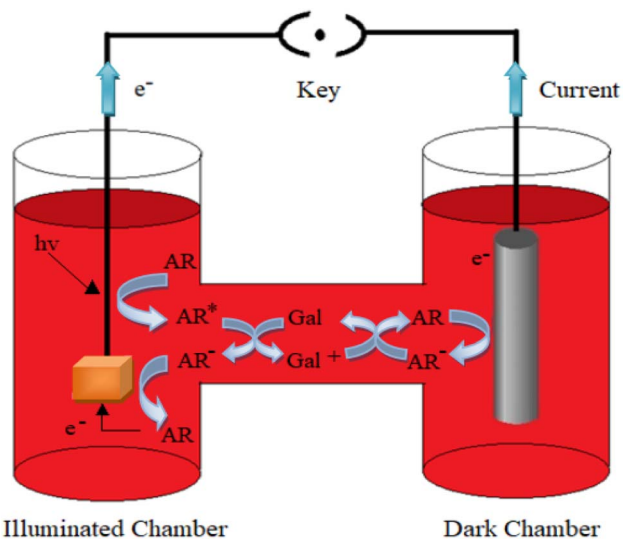

Fig. 2 Mechanism of photogeneration of the current. Here, $h\nu$, photon; Gal, D-galactose reductant molecule; Gal+, oxidized form of D-galactose reductant molecule; e, electron; AR-, Allura Red dye photosensitizer molecule; AR*, Allura Red molecule in excited state. Working electrode (Pt, Cu, Brass) in illuminated chamber, graphite counter electrode in dark chamber.

3rd Step: photophysical processes in the dark chamber and at the counter electrode: at the counter electrode (graphite) region, the dye molecule accepts an electron from the counter electrode and gets converted into the semi or leuco form. Finally, the leuco/semi form of the dye and oxidized form of the reductant combine to give the original dye (Allura Red) and reductant (D-galactose) molecules. This cycle goes on in the cell.

$$\text{Allura Red}^- + e^- \rightarrow \text{Allura Red}^- + \text{(semi or leuco) (at graphite electrode)} \quad (4)$$

$$\text{Allura Red}^- + \text{D-galactose}^+ \rightarrow \text{Allura Red} + \text{D-galactose} \quad (5)$$

Here, the Allura Red*, Allura Red$^-$, D-galactose and D-galactose$^+$ are the excited form of the dye (photosensitizer), semi or leuco form of the dye, and the reductant and its oxidized form, respectively. S, T and I_{sc} represent the singlet excited-state dye; triplet excited-state dye and intersystem crossing, respectively. This mechanism is diagrammatically represented in Fig. 2.

Table 1 Photogalvanics of copper working electrode (0.3 cm × 0.2 cm) in Allura Red-D-galactose-DDAC-NaOH electrolyte

	[Allura Red] [D-galactose] [DDAC][a]		
Cell parameter	Experiment 1	Experiment 2	Experiment 3
V_{dark} (mV)	433	335	424
V_{max} (mV)	730	760	697
V_{oc} (mV)	713	721	580
t (min)	15	15	12
I_{max} (μA)	7850	7900	5710
I_{sc} (μA)	4030	4360	4950
P_{pp} (μW)	552.3	529.0	536.5
V_{pp} (mV)	263	230	271
I_{pp} (μA)	2010	2300	1980
CE (%)	8.54	7.16	8.04
FF	0.19	0.16	0.18

[a] At [Allura Red] = 2.85×10^{-5} M; [D-galactose] = 1.42×10^{-4} M; [DDAC] = 1.42×10^{-3} M; Cu electrode size = 0.3 cm × 0.2 cm; Cu electrode area = 0.17 cm^2; light intensity = 7.299 mW cm^{-2}; graphite electrode = 4.1 cm × 0.3 cm; diffusion length [D_L] = 4.5 cm.

4. Results and discussion

The photogalvanics of the copper and brass electrodes in the Allura Red-D-galactose-DDAC photogalvanic system has been studied by constructing different cells. The study was done in two successive steps: first, the study of electrochemical properties of the copper and brass working electrodes under the same experimental conditions; and second, the step-comparison of the electrical data of copper and brass electrodes with the already published electrical data of the platinum electrode to select the most suitable electrode material for the photogalvanic cell. The results of the present study on the photogalvanics of the copper and brass electrodes in the Allura Red-D-galactose-DDAC photogalvanic system are described as follows.

4.1. Photogalvanics of copper working electrode

4.1.1. Photogalvanics of copper working electrode (0.3 cm × 0.2 cm). The main theme of the present research work is to study the electrochemical properties of the chemically different working electrodes (copper and brass) under the following electrolyte conditions: 0.5 ml of M/500 Allura Red-D dye with the final concentration of 2.85×10^{-5} M, 0.5 ml of M/100 D-galactose (reductant) with the final concentration of 1.42×10^{-4} M, 0.5 ml of M/10 didecyl dimethyl ammonium chloride (surfactant) with the final concentration of 1.42×10^{-3} M, pH 13.66, light intensity 7.299 mW cm^2, diffusion length (D_L) = 4.5 cm, and graphite electrode (cylindrical shape, length 4.1 cm × diameter 0.3 cm). A 1 N NaOH stock solution was prepared. Thereafter, 16 ml of this 1 N NaOH stock solution was used to make the electrolyte solution. The total volume of the electrolyte solution is 35 ml. The pH of this electrolyte solution is 13.66.

The experimental results for the copper electrode are presented in the Table 1 (first, second, and third experiments done under same conditions).

The observed electrical parameters in the first experiment for the copper electrode (0.3 cm × 0.2 cm) are as follows: dark potential, 433 mV; maximum potential, 730 mV; open-circuit potential, 713 mV; charging time (t), 15 min; maximum current, 7850 μA; short-circuit current, 4030 μA; maximum power, 552.30 μW; potential at power point, 263 mV; current at power point, 2010 μA; solar conversion efficiency, 8.54%; and fill factor, 0.19.

The observed electrical parameters in the second experiment for the copper electrode (0.3 cm × 0.2 cm) are as follows: dark potential, 335 mV; maximum potential, 760 mV; open-circuit potential, 721 mV; charging time (t), 15 min; maximum current, 7900 μA; short-circuit current, 4360 μA; maximum power, 529.00 μW; potential at power point, 230 mV; current at power point, 2300 μA; solar conversion efficiency, 7.16%; and fill factor, 0.16.

The observed electrical parameters in the third experiment for the copper electrode (0.3 cm × 0.2 cm) are as follows: dark potential, 424 mV; maximum potential, 697 mV; open-circuit potential, 580 mV; charging time (t), 12 min; maximum current, 5710 μA; short-circuit current, 4950 μA; maximum power, 536.58 μW; potential at power point, 271 mV; current at power point, 1980 μA; solar conversion efficiency, 8.04% and fill factor, 0.18.

4.1.2. Study of potential variation with time during illumination of the NaOH-Allura Red-D-galactose-DDAC-copper (0.3 cm × 0.2 cm) photogalvanic system. In the photogalvanic system of Allura Red-D-galactose-DDAC-copper, the H-cell is filled with a known amount of electrolyte solution (total volume 35 ml, consisting of the reductant, dye, surfactant, alkali, and water solvent). In the dark condition, the cell is allowed to attain equilibrium potential (stable potential), called dark potential (V_{dark}, observed 433 mV in the present case), while the circuit is open. Thereafter, the cell is charged by illuminating it with artificial light with the intensity of 7.299 mW cm^{-2} while keeping the circuit open. During illumination, the potential is observed at 5 minute time intervals. The observed potential at

Table 2 Study of potential variation with time during illumination for the NaOH-Allura Red-D-galactose-DDAC-copper (0.3 cm × 0.2 cm) photogalvanic system

Time (min)	0	5	10	12	15
Potential (mV)	432	423	721	730 (V_{max})	713 (V_{oc})

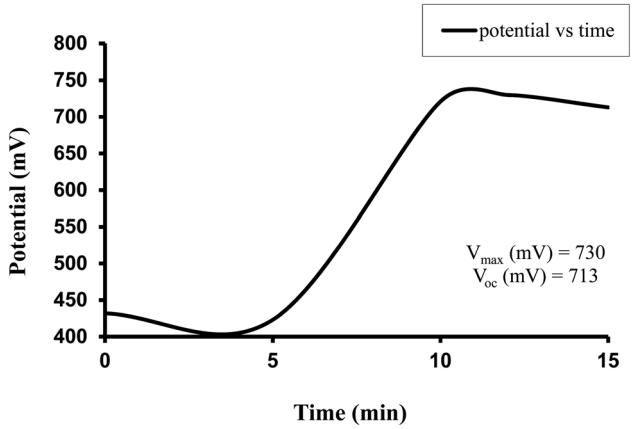

Fig. 3 Study of potential variation with time during illumination for the NaOH-Allura Red-D-galactose-DDAC-copper (0.3 cm × 0.2 cm) photogalvanic system.

zero time is 432 mV. On illumination, the potential rises and reaches the highest potential called maximum potential (V_{max}, 730 mV in present case); after some time, the potential goes down and attains a quasi-equilibrium potential (stable potential) called the open-circuit potential (V_{oc}, 713 mV in present case) (Table 2 and Fig. 3). The open-circuit potential (V_{oc}, 713 mV) was obtained after 15 minutes of continuous illumination. Therefore, in the present case, the time duration of 15 min was designated as the charging time of the cell.

4.1.3. Study of variation of current with potential (*I–V* characteristics of cell), and current with power, for the Allura Red-D-galactose-DDAC-copper (0.3 cm × 0.2 cm) photogalvanic system. The study of *I–V* characteristics of the cell represents the relationship between the voltage and the current flowing through it. It is one of the most common methods of determining how an electrical device functions in a circuit. In the present work, after fully charging the Allura Red-D-galactose-DDAC-copper photogalvanic system, the circuit is closed by a circuit key to observe the maximum current (I_{max}), 7850 μA at the external resistance (load) of zero. After some time, the current goes down marginally to a relatively stable value called equilibrium current (I_{eq}) or short-circuit current (I_{sc}), 4030 μA. The potential at (I_{sc}) is nearly zero. With the help of the potentiometer/rheostat, the resistance of the circuit is varied slowly from zero potential to maximum potential value, along with their corresponding current values, *i.e.*, from the short-circuit current value until the current is zero, to study the *I–V* characteristics of the cell (Table 3 and Fig. 4). The point in the *I–V* curve called the power point (P_{pp}), 552.3 μW, was determined where the product of potential and current was maximum.

For this Allura Red-D-galactose-DDAC-copper (0.3 cm × 0.2 cm) photogalvanic system, the value of the cell's electrical parameters obtained at the experimental conditions (temp. 34.7 °C, humidity 12%, electrolyte temp. 34.5 °C, pH of solution 13.66) is summarized as follows: dark potential, 433 mV; maximum potential (V_{max}), 730 mV; open-circuit potential (V_{oc}), 713 mV; charging time (min), 15 min; maximum current (I_{max}), 7850 μA; short-circuit current (I_{sc}), 4030 μA; power at power point (P_{pp}), 552.3 μW, current at power point (I_{pp}), 2010 mV, potential at power point (V_{pp}), 263 mV, fill factor (FF), 0.19, and conversion efficiency (CE) 8.54%.

4.1.4. Electrolyte composition variation for the photogalvanics of the copper working electrode (0.3 cm × 0.2 cm). The effect of variation of electrolyte composition in the Allura

Table 3 Study of variation of current with potential (*I–V* characteristics of cell), and current with power for Allura Red-D-galactose-DDAC-copper (0.3 cm × 0.2 cm) photogalvanic system[a]

Current (μA)	Potential (mV)	Power (μW)	Current (μA)	Potential (mV)	Power (μW)
4030	110	443.30	1210	321	388.41
3840	123	472.32	1120	324	362.88
3420	152	519.84	1050	330	346.50
3350	156	522.60	900	356	320.40
2010 (I_{pp})	263 (V_{pp})	552.30 (P_{pp})	820	373	305.86
1900	264	501.60	720	395	284.40
1800	269	484.20	610	425	259.25
1780	272	484.16	500	447	223.50
1700	277	470.90	410	462	189.42
1600	287	459.20	360	472	148.32
1540	295	454.30	240	488	117.12
1420	297	421.74	110	511	56.210
1320	307	405.24	000	534	000

[a] CE = 8.54%; FF = 0.19; dye = 0.5 ml of M/500; reductant = 0.5 ml of m/100; surfactant = 0.5 ml of m/10; pH = 13.66; Cu electrode size = 0.3 cm × 0.2 cm; Cu electrode area = 0.17 cm^2, graphite electrode = 4.1 cm × 0.3 cm; room temp. = 34.7; humidity = 12%; solution temp., 34.5; distance from the bulb = 8 cm; light intensity = 7.299 mW cm^{-2}; initial E.C. of solution = 119.1; initial TDS of solution = 59.5 ppm; final temp. of solution = 58.7 °C; final TDS of solution = 61.2 ppm; final E.C. of solution = 114.9.

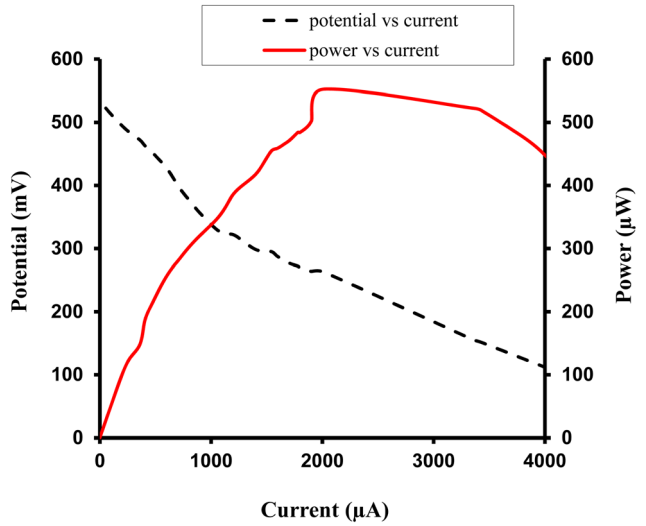

Fig. 4 Study of variation of current with potential (*I*–*V* characteristics of cell), and current with power for the Allura Red-D-galactose-DDAC-copper (0.3 cm × 0.2 cm) photogalvanic system.

Red-D-galactose-DDAC-copper (0.3 cm × 0.2 cm) photogalvanic system has been studied by constructing four photogalvanic cells (Table 4, Fig. 5 and Sec. 1 of ESI†). It has been observed in this study that the electrical power output for the second cell is highest. In the second cell, the dye, reductant, surfactant and NaOH show the highest cell performance at the optimal dye concentration of 0.57×10^{-5} M, reductant 0.28×10^{-4} M, surfactant 0.28×10^{-3} M, and NaOH pH 13.66.

The magnitude of the power (instead of the efficiency) was used to rate a cell as the best cell for the following reasons. Electrical generation plants are designed and built to provide power. Such plants are rated in watts, many megawatts usually.

Table 4 Electrolyte composition variation for the photogalvanics of the copper working electrode (0.3 cm × 0.2 cm)

Cell parameter	1st cell[a]	2nd cell[b]	3rd cell[c]	4th cell[d]
V_{dark} (mV)	362	391	433	423
V_{max} (mV)	746	764	730	720
V_{oc} (mV)	700	737	713	705
t (min)	10	10	13	10
I_{max} (μA)	7500	7670	7850	6290
I_{sc} (μA)	4440	4390	4030	3050
P_{pp} (μW)	611.2	621.6	552.3	522.9
V_{pp} (mV)	320	222	263	249
I_{pp} (μA)	1910	2800	2010	2100
CE (%)	9.65	9.61	8.54	10.24
FF	0.19	0.19	0.19	0.24

[a] 1st cell [dye 0.28×10^{-5} M, reductant 0.14×10^{-4} M, surfactant 0.14×10^{-3} M, NaOH pH 13.66]. [b] 2nd cell [dye 0.57×10^{-5} M, reductant 0.28×10^{-4} M, surfactant 0.28×10^{-3} M, NaOH pH 13.66]. [c] 3rd cell [dye 2.85×10^{-5} M, reductant 1.42×10^{-4} M, surfactant 1.42×10^{-3} M, NaOH pH 13.66]. [d] 4th cell [dye 8.5×10^{-5} M, reductant 4.28×10^{-4} M, surfactant 4.28×10^{-3} M, NaOH pH 13.66]; common for all cells: Cu electrode size = 0.3 cm × 0.2 cm, Cu electrode area = 0.17 cm^2, graphite electrode = 4.1 cm × 0.3 cm, light intensity = 7.299 mW cm^{-2}, diffusion length (D_L) = 4.5 cm, pH = 13.66.

They send out an amount of current at a certain voltage (Power = $I \times V$). Therefore, power output is the most important factor to determine how much electricity can be generated to meet the demands of a household or a commercial facility. Conversion efficiency, on the other hand, measures how effectively a cell converts input energy into useable output energy. It is a measure of the cell's effectiveness in utilizing the available resources. For solar cells, conversion efficiency indicates how much sunlight is converted into electricity.

4.1.5. Photogalvanics of the larger copper working electrode (1.0 cm × 1.0 cm). For the photogalvanics of the larger copper working electrode (1.0 cm × 1.0 cm), the electrolyte composition and other physical cell fabrication variables are the same as for the study of the photogalvanics of the smaller copper working electrode (0.3 cm × 0.2 cm).

The observed electrical parameters for the large copper working electrode (1.0 cm × 1.0 cm) are as follows: dark potential, 428 mV; maximum potential, 692 mV; open-circuit potential, 644 mV; charging time (t), 15 min; short-circuit current, 3520 μA; maximum current, 7100 μA; maximum power, 568.2 μW; potential at power, point 246 mV; current at power point, 2310 μA; solar conversion efficiency, 0.88; and, fill factor 0.25 (Table 5).

It has been observed in the study that different electrical power outputs were found for the different electrode areas. This shows that the electrode area affects the cell performance. It means the cell performance is electrode-area-dependent, and the cell shows the highest performance at some optimal electrode area due to different reasons.

It has been observed that the electrical power output (568.2 μW) for the large copper working electrode (1.0 cm × 1.0 cm) is higher than the electrical power output (552.3 μW) for the small copper working electrode (0.3 cm × 0.2 cm).

In the photogalvanic cell, the excited and reduced dye molecules collide with the working electrode, and through this process, the excess electron from the dye molecule is transferred to the working electrode. The number of electrons transferred per second from the dye to the copper electrode constitutes the current in the external circuit. How many dye molecules at a time may interact with the copper electrode depends on the electrode surface area. For a larger electrode area, the number of dye molecules interacting with copper electrode may be more, which will result in a higher electrical power compared to the smaller area.

4.2. Photogalvanics of the brass working electrode

4.2.1. Photogalvanics of the brass working electrode (0.3 cm × 0.2 cm). In the Allura Red-D-galactose-DDAC-brass photogalvanic system, each cell has 0.5 ml of M/500 Allura Red-D dye with resultant concentration 2.85×10^{-5} M; 0.5 ml of M/100 D-galactose (reductant) with resultant concentration 1.42×10^{-4} M; 0.5 ml of M/10 didecyl dimethyl ammonium chloride (surfactant) with resultant concentration 1.42×10^{-3} M; 16 ml of 1 N NaOH having resultant pH of 13.66; light intensity 7.299 mW cm^{-2}; diffusion length (D_L) = 4.5 cm; pH = 13.66; and graphite electrode (cylindrical shape, length 4.1 cm × diameter

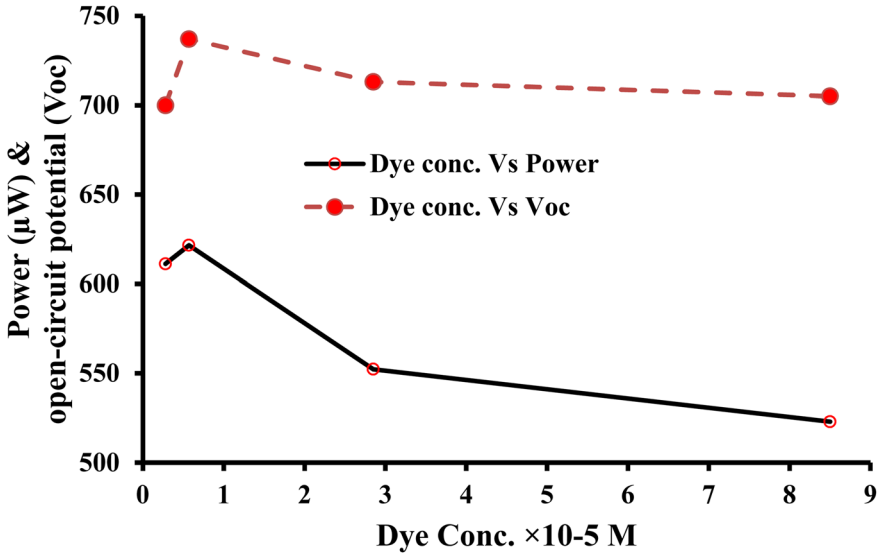

Fig. 5 Variation of power and open-circuit potential with dye concentration for photogalvanics of the copper working electrode.

Table 5 Photogalvanics of the larger copper working electrode (1.0 cm × 1.0 cm)

[Allura Red] [D-galactose] [DDAC][a]			
Electrical parameters of the cell			
V_{dark} (mV)	428	P_{pp} (μW)	568.2
V_{max} (mV)	692	V_{pp} (mV)	246
V_{oc} (mV)	644	I_{pp} (μA)	2310
t (min)	15	CE (%)	0.88
I_{max} (μA)	7100	FF	0.25
I_{sc} (μA)	3520		

[a] At [Allura Red] = 2.85×10^{-5} M; [D-galactose] = 1.42×10^{-4} M; [DDAC] = 1.42×10^{-3} M; Cu electrode size = 1.0 cm × 1.0 cm; Cu electrode area = 2.2 cm^2; graphite counter electrode = 4.1 cm × 0.3 cm; light intensity = 7.299 mW cm^{-2}; diffusion length [D_L] = 4.5 cm.

0.3 cm). The electrochemical property of the brass working electrode has been studied under the same experimental conditions as used for the copper electrode.

The experimental results for the brass electrode are presented in Table 6 and Fig. 6 (first, second, and third experiments done under same conditions).

The observed electrical parameters in the first experiment for the brass electrode (0.3 cm × 0.2 cm) are as follows: dark potential, 451 mV; maximum potential, 788 mV; open-circuit potential, 739 mV; charging time (t), 15 min; maximum current, 9200 μA; short-circuit current, 5320 μA; maximum power, 546.4 μW; potential at power point, 216 mV; current at power point, 2530 μA; solar conversion efficiency, 6.12%; and fill factor, 0.13.

The observed electrical parameters in the second experiment for the brass electrode (0.3 cm × 0.2 cm) are as follows: dark potential, 489 mV; maximum potential, 743 mV; open-circuit potential, 722 mV; charging time (t), 15 min; maximum current, 6000 μA; short-circuit current, 4810 μA; maximum power, 543.7 μW; potential at power point, 171 mV; current at power point, 3180 μA; solar conversion efficiency, 6.83%; and fill factor, 0.15.

The observed electrical parameters in the third experiment for the brass electrode (0.3 cm × 0.2 cm) are as follows: dark potential, 424 mV; maximum potential, 741 mV; open-circuit potential, 716 mV; charging time (t), 15; maximum current, 6180 μA; short-circuit current, 3950 μA; maximum power, 540.6 μW; potential at power point, 218 mV; current at power point, 2480 μA; solar conversion efficiency, 8.32%, and fill factor, 0.19.

In Section 4.1.1 for the copper electrode, and in this Section 4.2.1 for the brass electrode, the experiments were repeated three times under similar conditions to determine the reproducibility of the results for the copper and brass electrodes.

Table 6 Photogalvanics of the brass working electrode (0.3 cm × 0.2 cm) in Allura Red-D-galactose-DDAC-NaOH electrolyte

	[Allura Red] [D-galactose] [DDAC][a]		
Cell parameter	Experiment 1	Experiment 2	Experiment 3
V_{dark} (mV)	451	489	424
V_{max} (mV)	788	743	741
V_{oc} (mV)	739	722	716
t (min)	15	15	15
I_{max} (μA)	9200	6000	6180
I_{sc} (μA)	5320	4810	3950
P_{pp} (μW)	546.4	543.7	540.6
V_{pp} (mV)	216	171	218
I_{pp} (μA)	2530	3180	2480
CE (%)	6.12	6.83	8.32
FF	0.13	0.15	0.19

[a] At [Allura Red] = 2.85×10^{-5} M; [D-galactose] = 1.42×10^{-4} M; [DDAC] = 1.42×10^{-3} M; brass electrode size = 0.3 cm × 0.2 cm; brass electrode area = 0.17 cm^2; graphite electrode area = 4.1 cm × 0.3 cm; light intensity = 7.299 mW cm^{-2}; diffusion length (D_L) = 4.5 cm; pH = 13.66.

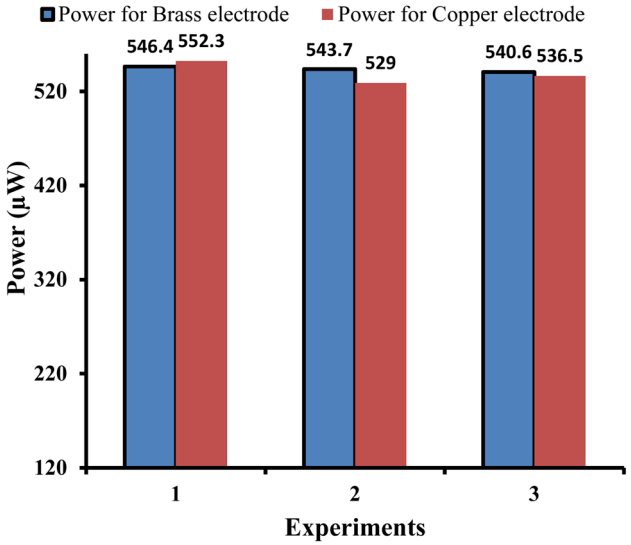

Fig. 6 Comparison of the power outputs of the copper and brass working electrodes in three similar experiments (reproducibility of the power output).

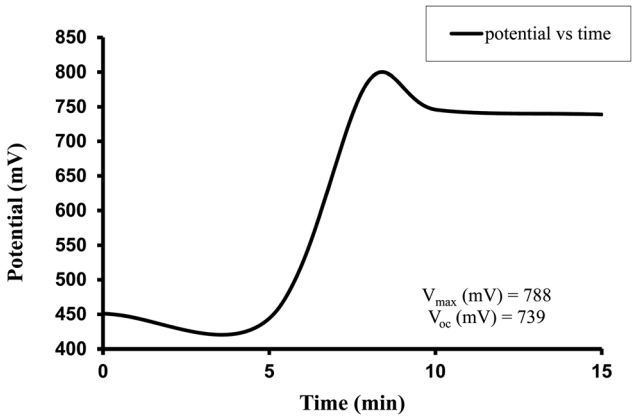

Fig. 7 Study of potential variation with time during illumination of the NaOH-Allura Red-D-galactose-DDAC-brass (0.3 cm × 0.2 cm) photogalvanic system.

It is observed that the electrical output of the cell is repeatable and reproducible with both electrodes (*i.e.*, copper and brass). It is obvious from the comparable (quite similar) electrical power output values observed in the three experiments for copper and brass electrodes, *i.e.*, the obtained power for the copper electrode is 552.30 μW, 529.00 μW, and 536.58 μW for the first, second, and third experiments, respectively. The obtained power for the brass electrode is 546.4 μW, 543.7 μW, and 540.6 μW for the first, second, and third experiments, respectively. Here, it is to be noted that some error (like measurement of solution, *etc.*) is inevitable while repeating the experiments leading to the minor variation in power output.

4.2.2. Study of potential variation with time during illumination of the NaOH-Allura Red-D-galactose-DDAC-brass (0.3 cm × 0.2 cm) photogalvanic system. In the dark condition, the cell filled with electrolyte is allowed to attain equilibrium potential (stable potential) called dark potential (V_{dark}, observed to be 451 mV in the present case) while circuit is open (Sec. 2 of ESI†). Thereafter, the cell is charged by illuminating it with artificial light with intensity 7.299 mW cm^{-2} while keeping the circuit open. During illumination, the potential is observed at time intervals of five minutes. The observed potential at zero time is 451 mV. Upon illumination, the potential rises and reaches a highest potential, called the maximum potential (V_{max}, 788 mV in present case), and after some time, the potential goes down and attains a quasi-equilibrium potential (stable potential) called the open-circuit potential (V_{oc}, 739 mV in present case; Table 7 and Fig. 7). The open-circuit potential (V_{oc}, 739 mV) was obtained after 15 minutes of continuous illumination. Therefore, in the present case, the time duration of 15 minutes was designated as the charging time of the cell.

Table 7 Study of potential variation with time during illumination of the NaOH-Allura Red-D-galactose-DDAC-brass (0.3 cm × 0.2 cm) photogalvanic system

Time (min)	0	5	8	10	15
Potential (mV)	451	444	788 (V_{max})	746	739 (V_{oc})

4.2.3. Study of variation of current with potential (*I–V* characteristics of cell), and current with power, for the Allura Red-D-galactose-DDAC-brass (0.3 cm × 0.2 cm) photogalvanic system. The *I–V* characteristics of the cell represent the relationship between the voltage and the current flowing through it. It is one of the most common methods of determining how an electrical device functions in a circuit. In the present work, after fully charging the Allura Red-D-galactose-DDAC-brass photogalvanic system, the circuit is closed by the circuit key to observe the maximum current (I_{max}) 9200 μA at the external resistance (load) of zero. After some time, the current goes down marginally to a relatively stable value called equilibrium current (I_{eq}), or short-circuit current (I_{sc}), of 5320 μA. The potential at (I_{sc}) is nearly zero. With the help of the potentiometer/rheostat, the resistance of the circuit is varied slowly from zero potential to maximum potential value along with their corresponding current values, *i.e.*, from the short-circuit current value until the current is zero, to study the *I–V* characteristics of the cell (Table 8 and Fig. 8). The point in the *I–V* curve called the power point (P_{pp}) 546.4 μW was determined where the product of potential and current was maximum.

For the Allura Red-D-galactose-DDAC-brass electrode (0.3 cm × 0.2 cm) photogalvanic system, the value of the cell's electrical parameters obtained at the experimental conditions (temp. 34.7 °C, humidity 12%, electrolyte temp. 33.8 °C, pH of solution 13.66) is summarized as follows: dark potential, 451 mV; maximum potential (V_{max}), 788 mV; open-circuit potential (V_{oc}), 739 mV; charging time (min), 15 min; maximum current (I_{max}), 9200 μA; short-circuit current (I_{sc}), 5320 μA; power at power point (P_{pp}), 546.4 μW; current at power point (I_{pp}), 2530 mV; potential at power point (V_{pp}), 216 mV; fill factor (FF), 0.13; and conversion efficiency (CE), 6.12%.

The error analysis has been correlated with the accuracy of the current and potential measurements by the digital

Table 8 Study of variation of current with potential (*I*–*V* characteristics of cell), and current with power, for the Allura Red-D-galactose-DDAC-brass (0.3 cm × 0.2 cm) photogalvanic system[a]

Current (μA)	Potential (mV)	Power (μW)	Current (μA)	Potential (mV)	Power (μW)
5320	62	329.8	1730	275	475.7
4320	84	362.8	1630	283	461.2
3580	122	436.7	1500	298	447.0
3510	130	456.3	1480	300	444.0
3490	133	464.1	1410	308	434.2
3400	140	476.0	1320	320	422.4
3310	150	496.5	1200	333	399.6
3280	153	501.8	1120	381	426.7
3200	159	508.8	1030	420	432.6
3130	170	532.1	950	540	513.0
3070	172	528.0	910	560	509.6
2910	185	538.3	870	574	499.3
2810	193	542.3	770	584	449.6
2770	197	545.6	720	598	430.5
2660	205	545.3	600	621	372.6
2530 (I_{pp})	216 (V_{pp})	546.4 (P_{pp})	560	632	353.9
2440	223	544.1	480	642	308.1
2300	236	542.8	420	663	278.4
2200	241	530.2	320	662	211.8
2110	249	525.3	230	680	156.4
2040	254	518.1	70	717	50.1
1950	262	510.9	000	733	000
1810	269	486.8			

[a] CE = 6.12%; FF = 0.13; dye = 0.5 ml of M/500; reductant = 0.5 ml of M/10; surfactant = 0.5 ml of M/100; pH = 13.66; brass electrode size = 0.3 cm × 0.2 cm; brass electrode area = 0.17 cm^2; graphite electrode = 4.1 cm × 0.3 cm; room temp. = 34.7; humidity = 12%; solution temp 34.5 = 33.8; distance from the bulb = 8 cm; light intensity = 7.299 mW cm^{-2}; E.C. = 113.1; TDS = 56.3 ppt.

multimeter. In this experiment, the Haoyue digital multimeters (model-DT830D UNITY) were used. The accuracy of measurements of the DC current and DC potential from this multimeter is ±2.0% and ±1.0%, respectively. Therefore, in the observation data in Table 8 and at other places in the manuscript, the error values of ±2.0%, ±1.0%, and ±3.0% are estimated in the measurement of the current, potential, and power of the cell.

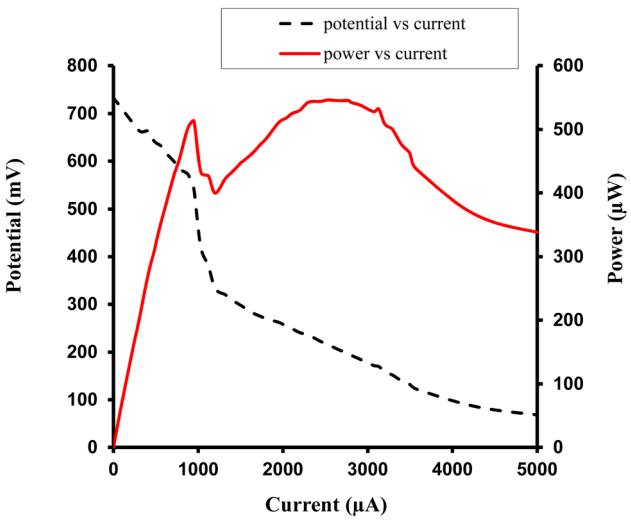

Fig. 8 Study of variation of current with potential (*I*–*V* characteristics of cell), and current with power, for the Allura Red-D-galactose-DDAC-brass (0.3 cm × 0.2 cm) photogalvanic system.

4.2.4. Electrolyte composition variation for the photogalvanics of the brass working electrode (0.3 cm × 0.2 cm). The effect of variation of electrolyte composition in the Allura Red-D-galactose-DDAC-brass (0.3 cm × 0.2 cm) photogalvanic system was studied by constructing four photogalvanic cells (Table 9; Sec. 3 of ESI†).

For electrical systems like solar cells, the power is indeed the product of measured current at a corresponding potential. Thus, power is a direct measurement, whereas the conversion efficiency is a calculated statistical measure. Both the fill factor and conversion efficiency are measures of cell performance. In the present set of four experiments, the chemical compositions (like concentration of dye, *etc.*) of the cells in all four different experiments are different. In first, second, third, and fourth experiments, the observed power (μW) and fill factor (FF) are 705.9 μW, 0.30; 637.2 μW, 0.26; 546.4 μW, 0.13; and 472.6 μW, 0.27; respectively. From the observations, it is clear that there is quite an appreciable difference in the fill factor values leading to the quite appreciable difference in efficiency data of the four experiments.

4.2.5. Photogalvanics of the larger brass working electrode (1.0 cm × 1.0 cm). For photogalvanics of the larger brass working electrode (1.0 cm × 1.0 cm), the electrolyte composition and other physical cell fabrication variables are same as for the study of the photogalvanics of the smaller brass working electrode (0.3 cm × 0.2 cm).

The observed electrical parameters for the larger brass working electrode (1.0 cm × 1.0 cm) are as follows: dark

Table 9 Electrolyte composition variation for the photogalvanics of the brass working electrode (0.3 cm × 0.2 cm)

Cell parameter	1st cell[a]	2nd cell[b]	3rd cell[c]	4th cell[d]
V_{dark} (mV)	371	339	457	439
V_{max} (mV)	763	733	788	719
V_{oc} (mV)	713	720	734	688
t (min)	10	20	20	10
I_{max} (μA)	6360	7830	9200	5900
I_{sc} (μA)	3290	3370	5320	2500
P_{pp} (μW)	705.9	637.2	546.4	472.6
V_{pp} (mV)	303	236	216	278
I_{pp} (μA)	2330	2700	2530	1700
CE (%)	17.06	13.45	6.12	10.43
FF	0.30	0.26	0.13	0.27

[a] 1st cell [dye 0.28×10^{-5} M, reductant 0.14×10^{-4} M, surfactant 0.14×10^{-3} M, NaOH pH 13.66]. [b] 2nd cell [dye 0.57×10^{-5} M, reductant 0.28×10^{-4} M, surfactant 0.28×10^{-3} M, NaOH pH 13.66]. [c] 3rd cell [dye 2.85×10^{-5} M, reductant 1.42×10^{-4} M, surfactant 1.42×10^{3} M, NaOH pH 13.66]. [d] 4th cell [dye 8.5×10^{-5} M, reductant 4.28×10^{-4}M, surfactant 4.28×10^{-3} M, NaOH pH 13.66]; common for all cells: brass electrode size = 0.3 cm × 0.2 cm; brass electrode area = 0.17 cm^2; graphite electrode = 4.1 cm × 0.3 cm; light intensity = 7.299 mW cm^{-2}; diffusion length (D_L) = 4.5 cm, pH = 13.66.

potential, 441 mV; maximum potential, 706 mV; open-circuit potential, 684 mV; charging time (t), 20 min; short-circuit current, 3300 μA; maximum current, 7430 μA; maximum power, 505.4 μW; potential at power point, 266 mV; current at power point, 1900 μA; solar conversion efficiency, 0.70%; and fill factor, 0.22 (Table 10).

Also, it has been observed that the electrical power output (546.4 μW) for the small brass working electrode (0.3 cm × 0.2 cm) is higher than the electrical power output (505.4 μW) for the large brass working electrode (1.0 cm × 1.0 cm). The better electrical output of the small electrode is due to the relatively less hindrance to diffusion of ions, as the photogalvanic cells are diffusion-controlled cells, depending on the diffusion of ions in the bulk of the electrolytic solution. Further, the larger brass electrode will affect the cell adversely due to steric hindrance in the diffusion path of the dye molecules.

The electrode properties of a material are dependent on its chemical, physical, electronic, and morphological properties. Therefore, the optimum size of the electrodes for optimum cell performance is supposed to be different for different electrode materials. Under similar electrolyte conditions, the optimum size of the copper electrode will be different than that for the brass electrode for optimum cell performance. This is due to the fact that the chemical and physical properties of the copper material are different than that for the brass material. Consequently, the different natures of copper and brass may be the reason for the different electrical power output for the copper and brass electrodes of the same sizes.

It has been observed that under similar experimental conditions, the electric power output for the copper electrode is relatively higher than that of the brass electrode. The reported electrochemical impedance spectroscopy study on the corrosion parameters of copper alloys (brass) in NaOH solution shows a higher value of charge transfer resistance, indicating lower electron release.[35] Further, it is also reported that copper metal in the NaOH solution has a lower transfer resistance value, indicating a higher electron release from the metal.[35] Hence, compared to brass (copper alloy), copper metal has a greater tendency to release electrons. These electrons migrate towards the circuit and will promote more passage of current.

Table 10 Photogalvanics of the larger brass working electrode (1.0 cm × 1.0 cm)

[Allura Red] [D-galactose] [DDAC][a]			
Electrical parameters of the cell			
V_{dark} (mV)	441	P_{pp} (μW)	505.4
V_{max} (mV)	706	V_{pp} (mV)	266
V_{oc} (mV)	684	i_{pp} (μA)	1900
t (min)	20	CE (%)	0.70
I_{max} (μA)	7430	FF	0.22
i_{sc} (μA)	3300		

[a] At [Allura Red] = 2.85×10^{-5} M; [D-galactose] = 1.42×10^{-4} M; [DDAC] = 1.42×10^{-3} M; brass electrode size = 1.0 cm × 1.0 cm; brass electrode area = 2.2 cm^2; light intensity = 7.299 mW cm^{-2}; graphite counter electrode = 4.1 cm × 0.3 cm; diffusion length [D_L] = 4.5 cm.

5. Comparison of the photogalvanics of copper, brass, and platinum working electrodes

The comparative photogalvanics of the chemically different working electrodes (*i.e.*, copper and brass) was studied under similar conditions of the cell fabrication variables. The difference is only in the chemical nature of the working electrodes. The photogalvanics of copper and brass working electrodes were compared at two dimensions, *i.e.*, 0.3 cm × 0.2 cm and 1.0 cm × 1.0 cm. Under similar experimental conditions, the electrical power outputs for both the small (0.3 cm × 0.2 cm)

Table 11 Comparison of the photogalvanics of copper and brass working electrodes (0.3 cm × 0.2 cm)

Cell parameter	Copper electrode[a] (0.3 cm × 0.2 cm)	Brass electrode[a] (0.3 cm × 0.2 cm)
V_{dark} (mV)	433	451
V_{max} (mV)	730	788
V_{oc} (mV)	713	739
t (min)	13	15
I_{max} (μA)	7850	9200
i_{sc} (μA)	4030	5320
P_{pp} (μW)	552.3	546.4
V_{pp} (mV)	263	216
i_{pp} (μA)	2010	2530
CE (%)	8.54	6.12
FF	0.19	0.13

[a] At [Allura Red] = 2.85×10^{-5} M; [D-galactose] = 1.42×10^{-4} M; [DDAC] = 1.42×10^{-3} M; pH = 13.66; copper and brass electrode size = 0.3 cm × 0.2 cm; copper and brass electrode area = 0.17 cm^2; light intensity 7.299 mW cm^{-2}; graphite electrode area = 4.1 cm × 0.3 cm; diffusion length [D_L] = 4.5 cm.

Table 12 Comparison of the photogalvanics of copper and brass working electrodes (1.0 cm × 1.0 cm)

Cell parameter	Copper electrode[a] (1.0 cm × 1.0 cm)	Brass electrode[a] (1.0 cm × 1.0 cm)
V_{dark} (mV)	428	441
V_{max} (mV)	692	706
V_{oc} (mV)	644	684
t (min)	15	20
I_{max} (μA)	7100	7430
i_{sc} (μA)	3520	3300
P_{pp} (μW)	568.2	505.4
V_{pp} (mV)	246	266
i_{pp} (μA)	2310	1900
CE (%)	0.88	0.70
FF	0.25	0.22

[a] At [Allura Red] = 2.85×10^{-5} M; [D-galactose] = 1.42×10^{-4} M; [DDAC] = 1.42×10^{-3} M; pH = 13.66; copper and brass electrode size = 1.0 cm × 1.0 cm; copper and brass electrode area = 0.17 cm^2; light intensity = 7.299 mW cm^{-2}; graphite electrode area = 4.1 cm × 0.3 cm; diffusion length [D_L] = 4.5 cm.

and the large (1.0 cm × 1.0 cm) copper electrode are relatively higher than those of the brass electrode (Tables 11 and 12). The reported electrochemical impedance spectroscopy study on the corrosion parameters of the copper alloy (brass) in NaOH solutions shows a higher value of charge transfer resistance, indicating lower electron release.[35] Further, it is also reported that copper metal in NaOH solution has a lower transfer resistance value, indicating higher electron release from the metal.[35] Hence, compared to brass (copper alloy), the copper metal has a greater tendency to release electrons.

The electrode properties of a material are dependent on its chemical, physical, electronic and morphological properties. Therefore, the optimum size of the electrodes for optimum cell performance is supposed to be different for different electrode materials. Under similar electrolyte conditions, the optimum size of the copper electrode will be different than that for the brass electrode for optimum cell performance. It is due to the fact that the chemical and physical properties of the copper material are different than those for the brass material. Consequently, the different natures of copper and brass may be the reason for the different electrical power output for the copper and brass electrodes of the same sizes.

It has been observed that under similar alkaline conditions, the electric power output for the copper electrode is relatively higher than that of the brass electrode. Further, the dissolution of both electrodes (copper as well as brass) was also observed in the present study, where the corrosion is correlated with the weight loss. The loss of the metal specimen during corrosion was tested by taking the weight of the metal electrode before and after each cycle of a 10-cycle experiment. Before the experiment, the weight of the copper electrode sized 0.3 cm × 0.2 cm was 2.037 g, and after the experiment, it was 1.934 g. Similarly, the weight of the brass electrode sized 0.3 cm × 0.2 cm before the experiment was 2.208 g, and after the experiment, it was 2.115 g. Whereas, no noticeable weight loss has been found in platinum due to its inert property.

In alkaline medium, the relative photogalvanics of the copper and brass electrodes can be explained on the basis of published studies.[35–38] The reported electrochemical impedance spectroscopy study on the corrosion parameters of copper alloys (brass) in NaOH solution shows a higher value of charge transfer resistance, indicating lower electron release from the brass electrode.[35] Further, it is also reported that the copper metal in NaOH solution has a lower transfer resistance value, indicating a higher electron release from the copper metal electrode.[35] Hence, compared to brass (copper alloy), the copper metal electrode has a greater tendency to release electrons and consequently higher capacity to show power output (552.3 μW for copper; 546.4 μW for brass).

Similarly, the dissolution of the copper and brass electrodes as observed in the present study in alkaline medium can be explained on the basis of published studies.[35–38] For copper in NaOH alkaline medium, four anodic peaks are reported corresponding to the successive formation of a monolayer of Cu_2O, a thick layer of CuO and CuO_2^{2-} and, finally, a higher oxide Cu_2O_3 before the evolution of oxygen.

The reported cyclic voltammetric study of the electrochemical behavior of copper material at various alkali concentrations shows the following most possible oxidation reactions of copper.[36]

$$Cu + OH^- \rightarrow Cu(OH^-) + e^- \quad (6)$$

$$2Cu(OH^-) \rightarrow Cu_2O + H_2O \quad (7)$$

$$Cu_2O + 2OH^- \rightarrow 2CuO + H_2O + 2e^- \quad (8)$$

$$Cu_2O + 2OH^- + H_2O \rightarrow 2Cu(OH^-)_2 + 2e^- \quad (9)$$

The resulting $Cu(OH^-)_2$ exists in the equilibrium: $Cu(OH^-)_2 \rightleftharpoons CuO + H_2O$

The cyclic voltammetric study of the electrochemical behavior of brass is also reported for the NaOH solutions. Two potential regions (the preferential and the simultaneous dissolution potential regions) are reported in the anodic portion of the voltammogram. In the first region, selective dissolution (dezincification) of the less noble zinc material occurs with appearance of two anodic peaks showing the formation of ZnO film of a duplex nature. In the second potential region, the simultaneous dissolution of both the zinc and copper materials occurs with the appearance of three anodic peaks showing the formation of Cu_2O, $Cu(OH)_2$, and CuO on the electrode surface, respectively. It is reported that alloying zinc with copper decreases the dissolution of zinc from the alloy. This behavior could be explained on the basis that the dissolution is limited by the non-steady-state diffusion of zinc atoms from the bulk of the alloy to the alloy solution interface, which implies that the rate-determining step of dezincification is the diffusion of zinc atoms. The process of preferential dissolution of zinc leads to

the formation of a layer rich in copper and depleted in zinc on the electrode surface.[37]

Because of the oxidation of brass and copper, the photogalvanic cell's electric output has been increased as a result of electrons lost from the electrode surface. When exposed to an alkaline solution, copper has been found to corrode (oxidise) more quickly than brass (copper alloy). The corrosion of brass, an alloy consisting of copper and zinc, is lower because there is no metal coupling effect.[38]

The electrochemical properties of the platinum electrode was also studied under the same experimental conditions as used for the copper and brass electrodes (Sec. 4 of ESI†) (Table 13).

Under similar experimental conditions, the observed electrical outputs of the copper, brass, and platinum working electrodes are 552.3 μW, 546.4 μW, and 443.8 μW, respectively. The comparison of the data under similar experimental conditions shows that the electrical outputs for the copper and brass electrodes are higher than the electrical output for the platinum working electrode.

The photogalvanic cells are based on the photogalvanic effect. The photogalvanic effect arises due to the photophysical processes occurring in the body of the electrolyte solution.[6–8] Therefore, the role of electrodes in photogalvanic cells is mainly to complete the electrical circuit and to efficiently facilitate electron exchange. Platinum bears all these properties. Platinum is an inert metal with very good electron exchange capacity. Therefore, the platinum electrode has been widely explored as a working electrode in photogalvanic cells.[15–18] However, platinum has some drawbacks, such as its high cost and unavailability in the local market. Its procurement is very costly and time-consuming. In contrast, copper metal and brass alloy materials are cheap and easily available even at the household level. Therefore, the procurement of copper metal and brass alloy is cheaper and less time consuming. One more additional advantage of copper and brass is that the electrical output for the copper- and brass-based cells is relatively higher than that for the platinum electrode-based cells.

6. Comparison of the present photogalvanics of copper and brass electrodes with the published photogalvanics of the platinum electrode

In the present study, the observed electrical power outputs for the photogalvanics of the copper and brass working electrode are 552.3 μW and 546.4 μW, respectively. The electrical power output reports for the photogalvanics of the platinum working electrodes are 158.72 μW,[39] 138.60 μW,[28] 174.2 μW,[41] 345.0 μW,[44] 367.8 μW,[17] 989 μW,[42] and 1170 μW[43] (Table 14).

The observed electrical power output for the photogalvanics of copper and brass is found relatively higher compared to most of the reported photogalvanics of the platinum electrode. Further, the observed electrical power outputs for the copper and brass electrodes are also found relatively lower compared to the some reported photogalvanics of the platinum electrode.

Table 13 Photogalvanics of platinum working electrode (0.3 cm × 0.2 cm) in Allura Red-D-galactose-DDAC-NaOH electrolyte

[Allura Red] [D-galactose] [DDAC][a]			
Electrical parameters of the cell			
V_{dark} (mV)	435	P_{pp} (μW)	443.8
V_{max} (mV)	726	V_{pp} (mV)	269
V_{oc} (mV)	721	I_{pp} (μA)	1650
t (min)	20	CE (%)	11.61
I_{max} (μA)	5510	FF	0.25
I_{sc} (μA)	2400		

[a] At [Allura Red] = 2.85×10^{-5} M; [D-galactose] = 1.42×10^{-4} M; [DDAC] = 1.42×10^{-3} M; Pt electrode size = 0.3 cm × 0.2 cm; light intensity 7.299 mW cm^{-2}; graphite electrode area = 4.1 cm × 0.3 cm; diffusion length [D_L] = 4.5 cm.

The higher electrical outputs of the copper and brass electrodes in comparison to the platinum electrode can be traced to the mechanism of photogeneration of the current from the photogalvanic cells and the electrochemical standard reduction potential of the platinum, copper and brass (alloy of copper and zinc) electrodes. From the mechanism, it is obvious that the migration of electrons from the working electrode towards the external circuit causes the flow of the current. A higher tendency of the working electrode to give electrons towards the circuit will also favor the current. The composition of the brass electrode is 66% Cu and 34% Zn. Therefore, the electrochemical nature of the Cu and Zn elements will decide the electrochemical nature of the brass electrode.

The standard reduction potentials for platinum (Pt^{2+}/Pt), copper (Cu^{2+}/Cu), copper (Cu^{2+}/Cu^{+}), and zinc (Zn^{2+}/Zn) are +1.2 V, + 0.34 V, + 0.15 V, and −0.76 V, respectively. From the electrochemical series, a higher standard reduction potential (more positive value) indicates a higher tendency to receive electrons (lower tendency to give electrons). So, the copper (Cu) and brass (Zn-Cu) working electrodes have a higher tendency to give electrons than the platinum (Pt) electrode. Therefore, the electrical current and power are relatively higher for copper (Cu) and brass (Zn-Cu) working electrodes than for the platinum (Pt) working electrodes.

Further, the electrical output of copper and brass electrodes is also supplemented by the use of a more effective counter electrode (*i.e.*, graphite in the present study) in place of the saturated calomel electrode used as counter/reference electrode in previous studies.

Moreover, platinum (Pt) is expensive, while copper (Cu) and brass (alloy of Cu and Zn) possess the lowest price compared to platinum (Pt).

The superior electrical and thermal conductivity of copper and brass materials, coupled with their inherent corrosion properties, ensures a reliable and efficient electron transfer process in the cell. Additionally, copper and brass are widely available and economically viable materials, making them sustainable for large-scale implementation. Further, copper and

Table 14 Comparison of present photogalvanics for the copper and brass electrodes with platinum electrode from published work

S. No.	Photogalvanic system: Working electrode used	Reference/counter electrode used	Dye-reductant-surfactant-NaOH	Electrical parameters of the cell: V_{max}	I_{max}	I_{sc}	Power (μW)	CE (%)	Year	Reference
1	Copper (0.3 × 0.2 cm^2)	Graphite	Allura Red (dye)-D-galactose (reductant)-DDAC (surfactant)-NaOH	730	7850	4030	552.3	8.54	Present study	
2	Copper (1.0 × 1.0 cm^2)	Graphite	Allura Red (dye)-D-galactose (reductant)-DDAC (surfactant)-NaOH	692	7100	3520	568.2	0.88	Present study	
3	Brass (0.3 × 0.2 cm^2)	Graphite	Allura Red (dye)-D-galactose (reductant)-DDAC (surfactant)-NaOH	788	9200	5320	546.4	6.12	Present study	
4	Brass (1.0 × 1.0 cm^2)	Graphite	Allura Red (dye)-D-galactose (reductant)-DDAC (surfactant)-NaOH	706	7430	3300	505.4	0.70	Present study	
5	Platinum (1.0 × 1.0 cm^2)	SCE	Rose bengal (dye)-D-xylose (reductant)-NaLS (surfactant)-NaOH	885.0	575	460.0	158.72	1.52	2010	39
6	Platinum (1.0 × 1.0 cm^2)	SCE	Methyl orange (dye)-D-xylose (reductant)-NaLS (surfactant)-NaOH	1085.0	625.0	480	427.20	1.6245	2011	40
7	Platinum (1.3 × 1.3 cm^2)	SCE	Safranine-O (dye)-EDTA (reductant)-NaLS (surfactant)-NaOH	871.8	400.0	200.0	174.2	0.7213	2013	41
8	Platinum (1.0 × 1.0 cm^2)	SCE	Fast green FCF (dye)-fructose (reductant)-NaOH	1083	431	380	138.60	1.33	2014	28
9	Platinum (0.4 × 0.2 cm^2)	SCE	Sudan-I (dye)-fructose (reductant)-NaOH	1020	1800	1350	367.8	11.49	2021	17
10	Platinum (0.2 × 0.15 cm^2)	Graphite	Quinoline yellow-cellobiose-DTAB-NaOH	902	10 000	8000	989	15.08	2022	42
11	Platinum (0.6 × 0.23 cm^2)	Graphite	Bromo cresol green (dye)-formaldehyde (reductant)-surfactant-NaOH	750	25 000	8000	1170	9.02	2022	43
12	Platinum (0.1 × 0.3 cm^2)	Graphite	Carmoisine A (dye)-Lactic acid (reductant)-CAPB (surfactant)-NaOH	731	5500	2500	345.0	25.4	2023	44

brass corrosion can be controlled by using corrosion inhibitors or by moulding with different metals that can resist corrosion for further studies. While alternative materials may have certain advantages, copper and its alloys' unique combination of properties makes them the most practical and reliable choice for enabling a sustainable future through solar power generation technologies.

7. Challenges in present work and suggestions for future

The major challenges faced in the present work are related to the dissolution of the copper and brass electrodes in the alkaline electrolyte. Future research on photogalvanic cells may plan to tackle these challenges of corrosion-induced electrode loss. In the present study, the copper and brass electrodes are slowly corroded by alkali.

This loss of copper and brass electrode material can be prevented by the use of inhibitors reported in the literature.[45] Different inhibitors are used for the protection of metals and their alloys. However, nowadays, researchers have focused on nontoxic and environmentally friendly inhibitors. Generally, leaf extracts and organic inhibitors are reported as more efficient inhibitors as compared to other inorganic and toxic inhibitors.[45] The corrosion inhibition by plant extracts is generally attributed to the existence of complex organic molecules, *e.g.*, tannins, alkaloids, nitrogen bases, carbohydrates, amino acids, and proteins. The polar functional groups with the heteroatoms (N, S, O), along with the conjugated double bonds or aromatic rings, create the major adsorption centers in these plant extracts. The main adsorption centers of these heterocyclic compounds are polar functionalities with N, S, or O atoms and alternate double bonds, along with the presence of aromatic rings in their chemical structure.[46] The organic inhibitors possess features like the presence of hetero atoms and/or double bonds, large surface area, active center, *etc.*, which upon adsorption on the metal surface will blanket a large area of the metal and thus isolate it from the aggressive ions present in the environment. Benzotriazole (BTA) is also reported as a corrosion inhibitor for copper and its alloys in acidic and alkaline solution, because of its high inhibition efficiency. Benzotriazole is an organic compound consisting of benzene and a triazole ring, whose formula is $C_6H_5N_3$. The presence of

nitrogen atoms in the triazole ring enables bonding with copper and is a basis for the inhibitive effect of BTA.[47] The benzotriazole can be either neutral, negatively charged (BTA^-) or protonated ($BTAH_2^+$) depending on the pH of the test solution. Due to the high pK_a (8.4) constant, *i.e.*, in acidic environment (at low pH), the molecule is predominantly in neutral or undissociated form (BTAH). As the pH increases towards alkalinity (low $pK_a = 1$), the deprotonation of the molecule increases, becoming present in the BTA^- form. Benzotriazole has been extensively used for inhibition of copper corrosion by forming a monolayer or multilayer protective barrier layer in aqueous solutions.[48] Various mechanisms, though some contradictory in nature, have been proposed for benzotriazole molecule adsorption or film formation on copper surface. Cotton *et al.* proposed the formation of the surface complex of Cu-BTAH during the immersion of copper in BTAH solution, where soluble copper ion is formed.[49] Cotton and Scholes postulated that a polymeric film of 50 Å thick BTA forms on copper covalently bonded by the replacement of the H atom from the N–H group and a coordination bonding involving a lone pair of electrons from one nitrogen atom.[50] The formation of linear polymeric Cu(I) BTAH structure was not limited to a monolayer but could grow to several thousand Å thick due to the transport of Cu(I) ions from the matrix of copper metal through the surface film.[51]

The compounds 2-amino-5-ethylthio-1,3,4-thiadiazole, 2-amino-5-ethyl-1,3,4-thiadiazole and 5-(phenyl)-4*H*-1,2,4-triazole-3-thiol are also good corrosion inhibitors, but due to their adverse effects on the environment, health and organisms in recent times, the focus of research is transferred to the inhibiting action of biological molecules or mixtures of natural compounds called "green inhibitors".[52] Graphene-based materials may also be used as photoanodes in future research.[53] The present work used graphite as counter electrode. To further enhance the electrical performance of the photogalvanics of the NaOH-Allura Red-D-galactose-DDAC electrolyte, the use of alternative counter electrodes like $NiSe_2/MoSe_2$@N-BCCSs,[54] double-shell N–C-in-Co/N–C electrocatalysts with nanorod- and rhombic dodecahedron-shaped hollow morphologies,[55] and $Co_6Mo_6C_2$/Co@NC,[56] zinc oxide (ZnO) materials,[57] and CuS or PbS deposited ZnO nanorods should be considered.[58]

8. Conclusion

In the present research, entirely new and unexplored chemically different working electrodes (copper and brass) in place of platinum have been exploited in photogalvanic cells. Photogalvanics has mainly focused on the costly and non-ubiquitous platinum working electrodes. In the present work, the photogalvanics of cheap and easily available copper and brass working electrodes has been studied with the twin objective of developing cheaper photogalvanic cells with enhanced electrical output. The observed results for photogalvanics of the copper working electrode-Allura Red photosensitizer-D-galactose reductant-DDAC surfactant, and the brass working electrode-Allura Red photosensitizer-D-galactose reductant-DDAC surfactant, include the power of 552.3 μW and efficiency of 8.54%, and the power of 546.4 μW and efficiency 6.12%, respectively. The observed electrical outputs for the photogalvanics of copper and brass electrodes are relatively higher than that of most reported platinum photogalvanics. The chemically active nature and favorable redox potentials of copper and brass materials may be one of the reasons for their enhanced electrical output. Despite the loss of copper and brass electrode material during production of the current, the photogalvanics of copper and brass provides a relatively more efficient and cheaper route for solar energy conversion and storage through photogalvanic cells. It has been observed that under similar experimental conditions, the electrical power outputs from both the small and large copper electrodes are relatively higher than that of the brass electrode. The reason for the higher power of the copper electrode may be its lower value of charge transfer resistance.

Considering the overall cell performance, cost effectiveness, and availability, the copper and brass electrodes are identified to be the best option for solar power generation through the photogalvanic cell. The drawback in the loss of copper and brass in photogalvanics may be checked in future research by using inhibitors.

Data availability

All data have been incorporated in the manuscript.

Author contributions

PK and JS contributed in every aspect of this research work, including the conception, design, acquisitions, experimentation, analysis, interpretation of data, original writing of manuscript, review of manuscript, editing and finalization of manuscript, *etc.* Additionally, PK also contributed as corresponding author, mentor and supervisor of the research work. All authors have approved the submitted version (including the final version).

Conflicts of interest

Authors declare that they have no conflict of interest, and no competing interest.

Acknowledgements

The authors thank the Department of Chemistry, Jai Narain Vyas University, Jodhpur, Rajasthan (India), for providing the necessary laboratory facilities. Jyoti Saren is also grateful to the University Grants Commission (UGC), New Delhi (India), for providing financial assistance (fellowship) under the UGC-JRF Scheme.

References

1 R. Chenni, M. Makhlouf, T. Kerbache and A. Bouzid, A detailed modeling method for photovoltaic cells, *Energy*, 2007, **32**, 1724–1730.

2 M. I. H. Ansari, A. Qurashi and M. K. Nazeeruddin, Frontiers, opportunities, and challenges in perovskite solar cells: a critical review, *J. Photochem. Photobiol., C*, 2018, **35**, 1–24.
3 O. A. Abdulrazzaq, V. Saini, S. Bourdo, E. Dervishi and A. S. Biris, Organic Solar Cells: A Review of Materials, Limitations, and Possibilities for Improvement, *Part. Sci. Technol.*, 2013, **31**(5), 427–442.
4 M. K. Nazeeruddin, E. Baranoff and M. Gratzel, Dye-sensitized solar cells: a brief overview, *Sol. Energy*, 2011, **85**(6), 1172–1178.
5 A. J. Nozik, Quantum dot solar cells, *Phys. E*, 2002, **14**(1–2), 15–120.
6 E. K. Rideal and E. G. Williams, The action of light on the ferrous iodine iodide equilibrium, *J. Chem. Soc., Trans.*, 1925, **127**, 258–269.
7 E. Rabinowitch, The photogalvanic effect I. The photochemical properties of the thionine-iron system, *J. Chem. Phys.*, 1940, **8**(7), 551–559.
8 E. Rabinowitch, The photogalvanic effect II. The photogalvanic properties of the thionine-iron system, *J. Chem. Phys.*, 1940, **8**(7), 560–566.
9 C. Battaglia, A. Cuevas and S. D. Wolf, High-efficiency crystalline silicon solar cells: status and perspectives, *Energy Environ. Sci.*, 2016, **9**, 1552–1576.
10 F. Lan, J. Ba and H. Wang, The preparation of oleylamine modified micro-size sphere silver particles and its application in crystalline silicon solar cells, *RSC Adv.*, 2018, **8**, 16866–16872.
11 K. M. Gangotri and R. C. Meena, Use of reductant and photosensitizer in photogalvanic cells for solar energy conversion and storage: oxalic acid–methylene blue system, *J. Photochem. Photobiol., A*, 2001, **141**, 175–177.
12 K. M. Gangotri and J. Meena, Role of Surfactants in Photogalvanic Cells for Solar Energy Conversion and Storage, *Energy Sources, Part A*, 2006, **28**(8), 771–777.
13 S. Madhwani, R. Ameta, J. Vardia, P. B. Punjabi and V. K. Sharma, Use of Fluorescein-EDTA System in Photogalvanic Cell for Solar Energy Conversion, *Energy Sources, Part A*, 2007, **29**(8), 721–729.
14 S. Pramila and K. M. Gangotri, Use of Anionic Micelles in Photogalvanic Cells for Solar Energy Conversion and Storage Dioctylsulfosuccinate-mannitol-safranine System, *Energy Sources, Part A*, 2007, **29**(13), 1253–1257.
15 P. Koli, Natural sunlight-irradiated Rhodamine B dye sensitised and surfactant-enhanced photogalvanic solar power and storage, *Int. J. Ambient Energy*, 2021, **42**(10), 1193–1199.
16 P. Koli, Y. Dayma and R. K. Pareek, Simultaneous electrochemical solar power generation and storage using metanil yellow-formic acid as a new sensitizer-reductant couple in photogalvanic cells, *RSC Adv.*, 2019, **9**, 7560–7574.
17 P. Koli, Sudan-I dye and Fructose chemicals based photogalvanic cells for electrochemical solar energy conversion and storage at low and artificial sun intensity, *Arabian J. Chem.*, 2021, **14**(2), 1–15.
18 P. Koli, Enhancing efficiency of Fast Green FCF–Fructose photogalvanic solar cell by using surfactant in natural sunlight, *Int. J. Ambient Energy*, 2019, **40**(8), 868–874.
19 K. Li, H. Zhen, L. Niu, X. Fang, Y. Zhang, R. Guo, Y. Yu, F. Yan, H. Li and Z. Zheng, Full-Solution Processed Flexible Organic Solar Cells Using Low-Cost Printable Copper Electrodes, *Adv. Mater.*, 2014, **26**(42), 7271–7278.
20 E. Fortin and D. Masson, Photovoltaic effects in Cu_2O-Cu solar cells grown by anodic oxidation, *Solid-State Electron.*, 1982, **25**(4), 281–283.
21 B. Li, T. D. Sullivan, T. C. Lee and D. Badami, Reliability challenges for copper interconnects, *Microelectron. Reliab.*, 2004, **44**(3), 365–380.
22 C. R. Raghavendra, K. Hasavimath and K. Naik, Study on effectiveness of heat pipe heat exchanger with copper tube cylinders, *Mater. Today: Proc.*, 2021, **39**, 800–804.
23 K. R. Genwa and A. Chouhan, Studies of effect of heterocyclic dyes in photogalvanic cells for solar energy conversion and storage: NaLS-ascorbic acid system, *J. Chem. Sci.*, 2004, **116**(6), 339–345.
24 K. R. Genwa and A. Chouhan, Role of heterocyclic dye (Azur A) as a photosensitizer in photogalvanic cell for solar energy conversion and storage: NaLS–ascorbic acid system, *Sol. Energy*, 2006, **80**(9), 1213–1219.
25 M. Kumari, R. B. Pachwarya and R. C. Meena, Studies of Dye Sensitization for Solar Energy Conversion into Electrical Energy in Congo Red EDTA System, *Energy Sources, Part A*, 2009, **31**(13), 1081–1088.
26 N. D. Henderson, *A Review of the Environmental Impact and Toxic Effects of DDAC*, Environmental Protection Division BC Environment Ministry of Environment, Lands and Parks Victoria, British Columbia V8 1X4, 1992.
27 K. R. Genwa and C. P. Sagar, Tween 60 – amido black 10B – ascorbic acid system: Studies of photogalvanic effect and solar energy conversion, *J. Chem. Eng. Mater. Sci.*, 2011, **2**(9), 140–148.
28 P. Koli, Solar energy conversion and storage: Fast Green FCF-Fructose photogalvanic cell, *Appl. Energy*, 2014, **118**, 231–237.
29 P. Koli and U. Sharma, Photochemical solar power and storage through photogalvanic cells: Comparing performance of dye materials, *Energy Sources, Part A*, 2017, **39**(6), 555–561.
30 P. Koli, Photogalvanic effect of natural photosensitizer (crude spinach extract) in artificial light for simultaneous solar power generation and storage, *Environ. Prog. Sustainable Energy*, 2018, **37**(5), 1800–1807.
31 K. K. Bhati and K. M. Gangotri, Photogalvanic conversion of solar energy into electrical energy by using NaLS–xylose–methylene blue system, *Int. J. Electr. Power Energy Syst.*, 2011, **33**(2), 155–158.
32 P. Koli, U. Sharma and K. M. Gangotri, Solar energy conversion and storage: Rhodamine B - Fructose photogalvanic cell, *Renewable Energy*, 2012, **37**(1), 250–258.
33 C. Mall, S. Tiwari and P. P. Solanki, Comparison of dye (oxazine and thiazine) materials as a photosensitizer for use in photogalvanic cells based on molecular interaction

with sodium dodecyl sulphate by spectral study, *J. Saudi Chem. Soc.*, 2019, **23**(1), 83–91.
34 P. Koli and A. Meena, Photo-stability of the Titan Yellow dye sensitized and Ethylenediaminetetraacetate photoreduced photogalvanic system, *Results Eng.*, 2023, **18**, 101209.
35 I. Zaafarany and H. Boller, Electrochemical behavior of copper electrode in sodium hydroxide solutions, *Curr. World Environ.*, 2009, **4**(2), 277–284.
36 F. H. Assaf, S. S. A. El-Rehim and A. M. Zaky, Cyclic voltammetric behaviour of alpha brass in alkaline media, *Br. Corros. J.*, 2001, **36**(2), 143–150.
37 M. Samina, A. Karim and A. Venkatachalam, Corrosion Study of Iron and Copper Metals and Brass Alloy in Different Medium, *J. Chem.*, 2011, **8**, S344–S348.
38 R. Soenoko, P. H. Setyarini, S. Hidayatullah, M. S. Ma'arif and F. Gapsari, Corrosion characterization of Cu-based alloy in different environment, *Metallurgy*, 2020, **59**(3), 373–376.
39 K. M. Gangotri and M. K. Bhimwal, Study the performance of photogalvanic cells for solar energy conversion and storage: Rose Bengal–D-Xylose–NaLS system, *Sol. Energy*, 2010, **84**(7), 1294–1300.
40 K. M. Gangotri and M. K. Bhimwal, A Study of the Performance of the Photogalvanic Cells for Solar Energy Conversion and Storage: Methyl Orange–D-Xylose–NaLS System, *Energy Sources, Part A*, 2011, **33**(22), 2058–2066.
41 P. Gangotri and K. M. Gangotri, Studies of the Micellar Effect on Photogalvanics: Solar Energy Conversion and Storage—EDTA-Safranine O-NaLS System, *Energy Sources, Part A*, 2013, **35**(11), 1007–1016.
42 M. Jonwal, P. Koli, Y. Dayma, R. K. Pareek and R. Kumar, Photogalvanics of Dodecyltrimethyl Ammonium Bromide-Quinoline Yellow-alkali: A solar energy conversion, storage, photostability, and spectral study, *Int. J. Energy Res.*, 2022, **46**(10), 13889–13907.
43 P. Koli, Y. Dayma, R. K. Pareek, R. Kumar and M. Jonwal, Modified and simplified photogalvanic cells: solar energy harvesting using bromo cresol green dye with different electrodes and cell dimensions, *J. Electroanal. Chem.*, 2022, **904**.
44 P. Koli, A. Charan, J. Saren and A. Meena, Exploratory insight into the contribution of chemical components of photo galvanic electrolyte towards potential, power and current of photo galvanic cells, *Results Chem.*, 2023, **6**, 101124.
45 K. W. Shinato, A. A. Zewde and Y. Jin, Corrosion protection of copper and copper alloys in different corrosive medium using environmentally friendly corrosion inhibitors, *Corros. Rev.*, 2020, **38**(2), 101–109.
46 N. Chaubey, Savita, A. Qurashi, D. S. Chauhan and M. A. Quraishi, Frontiers and advances in green and sustainable inhibitors for corrosion applications: a critical review, *J. Mol. Liq.*, 2021, **321**, 114385.
47 M. M. Antonijevic and M. B. Petrovic, Copper Corrosion Inhibitors. A review, *Int. J. Electrochem. Sci.*, 2008, **3**(1), 1–28.
48 P. F. Khan, V. Shanthi, R. K. Babu, S. Muralidharan and R. C. Barik, Effect of benzotriazole on corrosion inhibition of copper under flow conditions, *J. Environ. Chem. Eng.*, 2015, **3**(1), 10–19.
49 I. Dugdale and J. B. Cotton, An electrochemical investigation on the prevention of staining of copper by benzotriazole, *Corros. Sci.*, 1963, **3**(2), 69–74.
50 J. B. Cotton and I. R. Scholes, Benzotriazole and Related Compounds as Corrosion Inhibitors for Copper, *Br. Corros. J.*, 1967, **2**(1), 1–5.
51 K. F. Khaled, M. A. Amin and N. A. Al-Mobarak, On the corrosion inhibition and adsorption behavior of some benzotriazole derivatives during copper corrosion in nitric acid solutions: a combined experimental and theoretical study, *J. Appl. Electrochem.*, 2010, **40**, 601–613.
52 M. V. Tomić, M. G. Pavlović, M. Jotanović and R. Fuchs-Godec, Protection of Copper and its Alloys Using Corrosion Inhibitor-Literature Review, *Quality of Life*, 2010, **1**(1).
53 E. Muchuweni, B. S. Martincigh and V. O. Nyamori, Recent advances in graphene-based materials for dye-sensitized solar cell fabrication, *RSC Adv.*, 2020, **10**, 44453–44469.
54 S. Yun, Z. Gao, T. Yang, M. Sun, G. Yang, K. Wang, Z. Wang, S. Yuan and M. Zhang, Constructing $NiSe_2/MoSe_2$ Mott–Schottky Heterojunctions Onto N-doped Brain Coral-Carbon Spheres by Phase Separation Strategies for Advanced Energy Conversion Applications, *Adv. Funct. Mater.*, 2023, 2314226, DOI: **10.1002/adfm.202314226**.
55 J. Dang, S. Yun, Y. Zhang, J. Yang, Z. Liu, C. Dang, Y. Wang and Y. Deng, Constructing double-shell structured N-C-in-Co/N-C electrocatalysts with nanorod and rhombic dodecahedron-shaped hollow morphologies to boost electrocatalytic activity for hydrogen evolution and triiodide reduction reaction, *Chem. Eng. J.*, 2022, **449**, 137854.
56 D. Qiao, S. Yun, M. Sun, J. Dang, Y. Zhang, S. Yuan, G. Yang, T. Yang, Z. Gao and Z. Wang, 1D/3D trepang-like N-modified carbon confined bimetal carbides and metal cobalt: Boosting electron transfer via dual Mott-Schottky heterojunctions triggered built-in electric fields for efficient hydrogen evolution and tri-iodide reduction, *Appl. Catal., B*, 2023, **334**, 122830.
57 A. Wibowo, M. A. Marsudi, M. I. Amal, M. B. Ananda, R. Stephanie, H. Ardy and L. J. Diguna, ZnO nanostructured materials for emerging solar cell applications, *RSC Adv.*, 2020, **10**, 42838–42859.
58 M. Eskandari, R. Ghahary, M. Shokri and V. Ahmadi, Zinc oxide/copper sulfide nanorods as a highly catalytic counter electrode material for quantum dot sensitized solar cells, *RSC Adv.*, 2020, **10**, 42838–42859.